

Synthesis, Characterization and Biological Activities of Schiff's Base Metal Complexes Derived from Hydroxy Trizene and Aromatic Aldehyde

A. S. Shekhawat, N. P. Singh, N. S. Chundawat*

Department of Chemistry; Bhupal Nobles' University; Udaipur-313002 (Rajasthan), India

Received 11 July 2021, accepted in final revised form 6 November 2021

Abstract

Schiff's bases are one of the important classes of the ligands, which are obtained by the condensation of amine and aromatic aldehyde. The metal complexes of Schiff's bases are widely considered because they show excellent biological activities. Such as antimicrobial, antitumor, antibacterial, and anti-fungal properties. The present studies deal with synthesis and characterization of Schiff's base transition metal complexes synthesized from general formula (ML) M=Co(II) and Cu(II); L = Schiff's base ligand derived from hydroxy trizene and aromatic aldehyde. The Synthesized complexes were characterized by physical and spectral analysis such as FTIR, ¹HNMR, and XRD. They were also tested in vitro biological activities. The Schiff base behaves as a bidentate ligand with O and N donors and binds to metal ions via hydroxy group oxygen and azomethane nitrogen. The Schiff's base ligands and Metal complexes' structure was confirmed by modern instrumental techniques viz, FTIR and ¹HNMR. The in-vitro antibacterial studies were carried out against *S. aureus*, *E. coli*, and *P. Aeruginosa* and anti-fungal activities *C.albicans*, *A. clavatus*. The result shows that the complexes have excellent biological activities.

Keywords: Schiff's base; Aromatic aldehyde; Metal salt; Antibacterial; Ethanol.

© 2022 JSR Publications. ISSN: 2070-0237 (Print); 2070-0245 (Online). All rights reserved.

doi: <http://dx.doi.org/10.3329/jsr.v14i1.54814>

J. Sci. Res. **14** (1), 387-394 (2022)

1. Introduction

The synthesis of imines has been reviewed many times in recent years. Schiff's bases are formed by condensing a primary amine and a carbonyl compound and were first reported by Hugo Schiff in 1864 [1]. Schiff's bases are generally bi- or tridentate ligands competent and very stable complexes with transition metals. In organic reactions, Schiff's base reactions are useful in making carbon-nitrogen bonds. Most Schiff's base complexes show excellent catalytic activity in various reactions at high temperatures [>100 °C]. Abundant scientific articles related to the catalytic activities of Schiff's base complexes. The interest in the polymerization of olefins has increased recently due to the observed catalytic activity of Schiff's base complexes in the synthesis of commercially value-added compounds [2-5]. The Schiff's bases form complexes with p-block and d-block metals, and these complexes have been known to act as highly efficient catalysts in various

* Corresponding author: chundawat7@yahoo.co.in

syntheses and other useful reactions. Many of Schiff's base complexes of ruthenium and palladium are used as catalysts in the synthesis of quality polymers [6,7]. Schiff's base ligands with oxygen or nitrogen donor atoms are a good class of organic compounds capable of binding to different metal ions with interesting medical and non-medical properties and very popular in the last decade [8]. Previously a number of biologically important complexes have been reported by researchers. [9,10]. In order to broaden the scale of investigations on the Schiff's bases, the present paper records the synthesis and characterization of Cu(II) and Co(II) complexes derived from 1-(4-amino-4 phenyl) 3-phenyl triazene-1-ol (hydroxy trizene), and aromatic aldehyde. The structures of the ligand and its metal complexes were characterized by IR and ^1H NMR. Schiff's base is reported to show a wide range of pharmacological activities [11]. Schiff's base complexes have been used as drugs and have valuable antibacterial, anti-fungal, antiviral, anti-inflammatory, and antitumor activities. Besides these, they also bear strong catalytic activity in various chemical reactions in chemistry and surfactant activities and as memory storage devices in electronics.

In the present paper, we have focused on synthesizing novel Schiff's base ligand by condensing aromatic aldehyde and its metal complexes with cobalt(II) and copper(II) salts. The coordination behavior of the ligand towards transition metal ions has been fully investigated by various spectral techniques. In continuation of our antibiotic research, we have also evaluated the antibacterial activities of ligands and their metal complexes against *S. aureus*, *S. pyogenes*, *E. coli*, *P. Aeruginosa*, and Fungal strains *C. albicans*, *A. clavatus* were chosen based on their clinical and pharmacological importance [12,13].

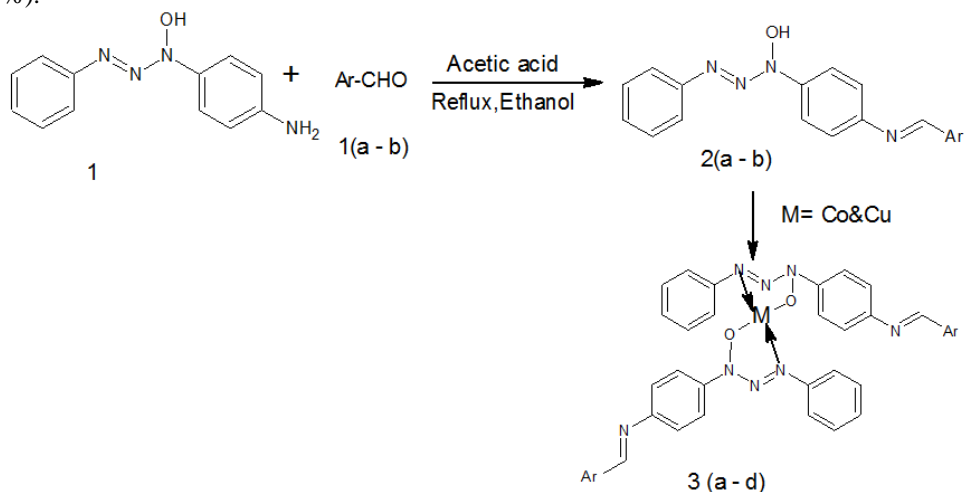
2. Material and Methods

All the chemicals used were of analytical reagent grade (AR) and maximum purity available. All reagents were commercially available. Solvents were purified and dry according to the standard procedures. Material source: Aldehyde (Spectrochem) and metal Cu(II), and Co(II) (Aldrich). FTIR spectra of the structures were recorded in KBr pellets with a Shimadzu FT-IR Spectrophotometer in the 4000-400 cm^{-1} range. The ^1H NMR spectra were measured at JEOL II 400 MHz from Delhi University, Delhi. XRD Rigaku (Model no-Mini Flex 600) and melting points are examined in open capillary tubes.

2.1. General procedure for the synthesis of Schiff's base ligands (2a-2b)

The Schiff's base ligands were synthesized by the following process. 0.1 mole of 1-(4-amino-4 phenyl) 3-phenyl triazene-1-ol (hydroxy trizene) was dissolved in absolute alcohol (50 mL) and added one drop of acetic acid. Slowly added to the solution of aromatic aldehyde (0.1 mol) in absolute alcohol (30 mL). The resulting mixture was maintained for 2-3 h at temperatures 75-80 $^{\circ}\text{C}$. The solution turned yellow to brownish. The progress of the reaction was checked by TLC. After completion of the reaction, the reaction mass was cooled and filtered off the product, followed by washing it 2-3 times with ice-cold water. Crystallization was carried out to obtain the purest products by using

absolute alcohol. The final products were obtained with crystal nature, the yield (70-80 %).



Scheme 1. Structure of Schiff's base ligands and its metal complexes.

2.2. General synthesis process for solid metal complexes (3a-3d)

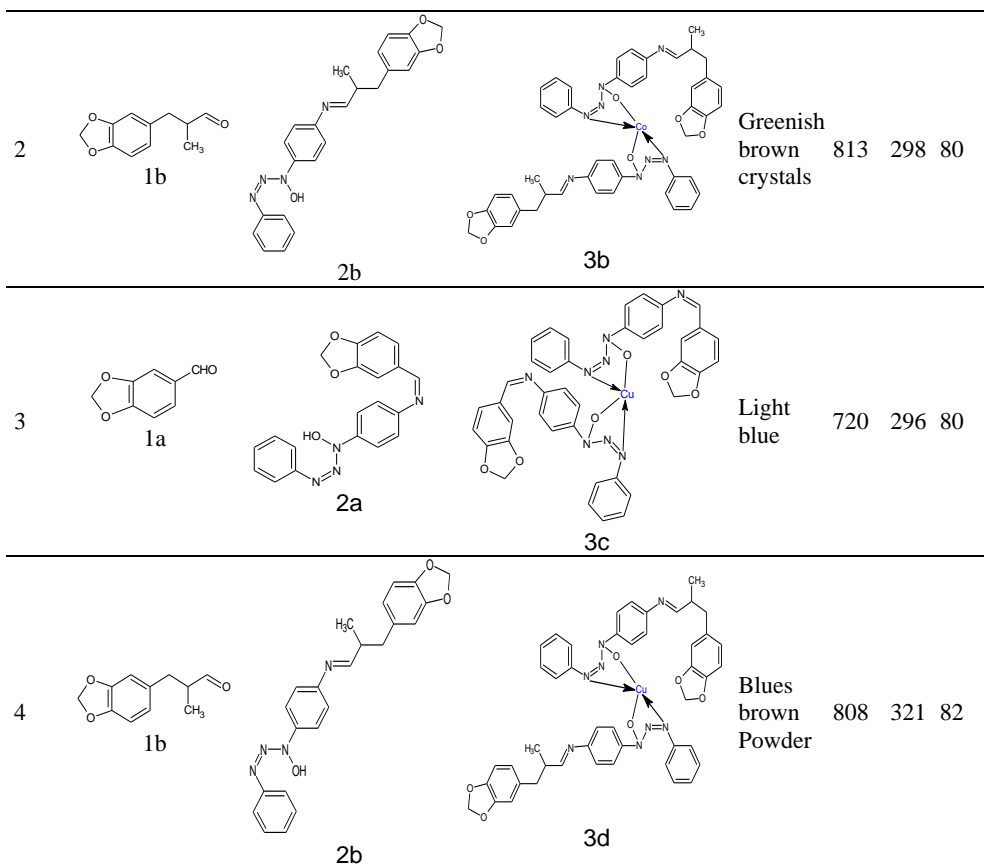
The metal complex's synthesis follows as a charged metal salt aqueous solution (M/1000) 5 mL in a round bottom flask equipped with a magnetic stirrer. Dropwise addition of an ethanolic solution of Schiff's base (M/1000) 20 mL was carried out at ambient temperature. (30-32 °C.) Maintained pH-4-5 by adding hexamine buffer solution. This reaction mixture was refluxed for 5 h. Cool reaction mass, filtered and washed with ethanol.

Solid metal complex obtained in the yield of 80-85 %

All Schiff's bases ligands and their metal complexes are novel and have not been reported in the literature. Physical characteristics and structures are tabulated as per Table.1.

Table 1. Schiff's base ligands and their metal complexes.

Entry	Reagent (Ar)	Ligands	Metal complexes	Color and shape	M.W.	M.P.	Yield (%)
1				Light brown powder	725	305	85



3. Result and Discussion

Typically, the metal complexes were obtained under reflux of respective metal salt with ligand (2a-2b) in a 1:2 mole ratio. The purity of the ligands (2a-2b) and metal complexes (3a-3d) obtained were checked by TLC, IR, ¹HNMR, and melting point. The proposed structure for ligand and its complexes are represented in scheme-01. FTIR spectroscopy gives formation on molecular vibrations or precision in the transitions between vibrational and rotational energy levels in molecules. Absorption bands detected in the region of 1700-1650 cm⁻¹ confirm the presence of (>C=N-) Schiff's base moiety, respectively, where the band wide at 3480 cm⁻¹ confirms the presence of hydrogen bond ν (O-H) stretching vibration. Comparison of the IR spectrum of the ligand with the metal complexes is observed in the range 3400-3600 cm⁻¹ which shows the absence of O-H stretching frequency in the metal complexes [14,15].

3.1. Physical characterization

The physical properties and the microanalytical data of the ligand and metal complexes are summarized in the experimental section. The analytical results show (1:2) metal-ligand ratio, that is, ML₂ type. The color change from ligand to metal complexes supports metal-ligand interaction, which is further reinforced by conductivity and pH change. The ligand was soluble in ethanol. The complexes were soluble in ethanol/acetone. The pH of ligand and complexes was almost in the neutral range.

3.2. Spectral characterization

IR spectroscopy gives formation on molecular vibrations or precision in the transitions between molecules' vibrational and rotational energy levels. Absorption bands detected in the region of 1700-1650 cm⁻¹ confirm the presence of (>C=N-) Schiff's base moiety, respectively, where the band wide at 3480 cm⁻¹ confirms the presence of hydrogen bond ν (O-H) stretching vibration. Comparison of the IR spectrum of the ligand with the metal complexes is observed in the range 3400-3600 cm⁻¹ which shows the absence of O-H stretching frequency in the metal complexes. The FTIR spectrum is also in line with the proposed ligand structure, with characteristic stretching vibrations at 1642 cm⁻¹ corresponding to the azomethane group. A Broadband with an absorption maximum of 3300 cm⁻¹ is possibly due to the collapse of N-H and O-H stretching peaks. The ¹HNMR spectrum of ligand executes a sharp singlet at 9.05 ppm corresponding to azomethane proton. On complexation, ν (C=N) stretching band for ligand has shifted to a lower absorption frequency of 1631 cm⁻¹ (3a) and 1624 cm⁻¹ (3b), showing the coordination of azomethine nitrogen atom to the metal ion. This shift toward the lower frequency of the azomethine group in the complexes is due to the decrease in electron density and force constant of the metal with the azomethine nitrogen lone pair. In all the complexes, FTIR absorption bands corresponding to ν (O-H) execute in 3337-3417 cm⁻¹ relative to 3300 cm⁻¹ for ligand. The evidence of bonding in 3(a-d) is also shown by the observation of new bands in the lower frequency regions at 423 and 523 cm⁻¹ characteristics to ν (Co-N) and ν (Co-O) stretching vibrations that are not observed in the IR spectrum of ligand.

The copper complex (3a-3b) executes a strong azomethine band at 1634 cm⁻¹ which has undergone a negative shift by 4 cm⁻¹ relatives to that of the free ligand. The other significant FTIR bands are observed at 442 cm⁻¹ ν (Cu-N). Its formation was strongly evidenced by FTIR and ¹HNMR spectral data. The strong azomethine band at 1629 cm⁻¹ ν (CH=N) for this complex has shifted by 11 cm⁻¹ towards a lower wavenumber relative to that of the free ligand, indicating metal coordination with azomethine nitrogen. The metal nitrogen coordination is further evidenced by a sharp peak at 414 cm⁻¹ in the FTIR spectrum of 3b. The ¹HNMR spectrum is also consistent with the suggested structure. The downfield shift of ¹HNMR signal for azomethine proton from δ 9.05 ppm for the ligand to δ 9.29 ppm for copper complex (3a-3d) also supports coordination of the azomethine nitrogen to the Cu (II) ion. Multiplet observed at δ 6.718-7.625 for ligand and δ 6.72-7.66 ppm for Cu (II) (3a-3d) are attributed to aromatic ring protons. The methyl protons of

ligand in both ligand and 1d appear as a singlet peak in the region of δ 1.118–1.562 ppm, which is still present in the ^1H NMR spectrum of Cu (II) and Co (II) complex (3a-3d) [16-18].

3.3. XRD data

During powder X-ray diffraction analyses, Co (II) and Cu (II) complexes of different Schiff's base Metal complexes (3a-3d) exhibited sharp peaks at Co (II) are crystalline in nature. In Co (II) complexes, the line broadening of the crystalline diffraction peak was relatively higher. By comparing diffractograms of the ligand with complexes, the crystalline nature of the complexes was indicated. This can be due to the inclusion of water molecules in the coordination sphere based on literature. Although the most accurate source of information regarding the complex structure is single-crystal X-ray crystallography, the difficulty of obtaining appropriate symmetric shapes of crystals makes this method unfit for such study.

4. Antimicrobial Activities [19-21]

Bacteria strains Gram-positive bacteria as *S. aureus* and *S. Pyogenes*, Gram-negative bacteria as *E. coli* and *P. aeruginosa*, and Fungal strains *C. albicans* and *A. clavatus* are selected based on their clinical pharmacological importance. Bacterial microbes were prepared in agar / YEPD genetics using a plate-spreading process. The fungal stock culture was placed 24 h at 37 °C in a potato dextrose agar (PDA) medium (Micro care laboratory, Surat, India), following refrigeration at 4 °C. Bacterial species were grown on Mueller-Hinton agar (MHA) plates at 37 °C (bacteria were planted in nutrient broth at 37 °C and stored in agar slants at 4 °C), while yeast and fungi were planted in Sabouraud dextrose agar (SDA) and in the PDA media, respectively, at 28 °C. Standard cultures were maintained at 4 °C.

Determination of zone of inhibition method: *In vitro* antibacterial and anti-fungal activities were tested on a sample. Activities of a sample against two Grams (+), two Grams (-), and two fungi have been investigated by the distribution of the agar disk diffusion method. Each sample was diluted with dimethyl sulfoxides, sterilized by filtration using a sintered glass filter, and stored at 4 °C. By determining the prevention area, Gram-positive, Gram-negative, and fungal species were treated as standard antibiotics. All compounds were tested for their antibacterial and anti-fungal activities against Gram-positive *S. aureus*, *S. Pyogenic*, and Gram-negative *E. coli*, *P. aeruginosa*, and fungal strains *A. clavatus* and *C. albicans*. Dilution (25 $\mu\text{g}/\text{mL}$) of the sample and standard drugs (5, 25, and 50 $\mu\text{g}/\text{mL}$) were prepared in double-distilled water using nutritious agar tubes. Mueller-Hinton's sterile agar plates were infected with bacterial infections (108 cfu) and allowed to remain at 37 °C for three hours. Control tests were performed under the same conditions using Cefixime and Griseofulvin as standard drugs. Growth inhibition zones around discs were rated after 18 to 24 h incubation at 37 °C in bacteria and 48 to 96 h for fungus at 28 °C (including disk width) on the surface of the

agar around the discs and values < 8 mm were considered as not active. Antibacterial and anti-fungal activities of both Schiff bases are tabulated in Tables 2 to 4.

Agar diffusion test (Mueller-Hinton test): It is a test that uses antibiotic -impregnate wafers to test whether certain bacteria are susceptible to certain antibiotics. A known number of bacteria are planted on agar plates in the presence of small wafers with appropriate antibiotics. When certain antibiotics attack bacteria, the cleaning area around the wafer where bacteria cannot grow is called the zone of inhibition.

Table 2. Antibacterial and fungal activity of ligands and metal complexes.

Group	Concentration ($\mu\text{g/mL}$)	Zone of inhibition in mm			
		<i>Staphylococcus aureus</i>	<i>Streptococcus Pyogenes</i>	<i>E. coli</i>	<i>P. Aeruginosa</i>
2a	25	13	13	12	14
2b	25	14	15	16	13
3a	25	18	18	22	16
3b	25	16	19	18	15
3c	25	18	17	20	16
3d	25	15	19	18	16
Anti-fungal activity					
		<i>Candida albicans</i>		<i>Aspergillus clavatus</i>	
3a	25	20		20	
3b	25	23		22	

Table 3. Antibacterial activity of standard antibacterial.

Standard Drug	Concentration ($\mu\text{g/mL}$)	Microorganisms zone of inhibition in mm			
		<i>Staphylococcus aureus</i>	<i>Streptococcus Pyogenes</i>	<i>Escherichia Coli</i>	<i>Pseudomonas aeruginosa</i>
	5	22	19	18	20
Cefixime	25	29	26	25	28
	50	33	35	36	37

Table 4. Anti-fungal activity of standard anti-fungal drugs.

Standard drug	Concentration ($\mu\text{g/mL}$)	Microorganisms zone of inhibition in mm	
		<i>Candida Albicans</i>	<i>Aspergillus clavatus</i>
Griseofulvin	5	34	35
	25	47	43
	50	52	55

4. Conclusion

Synthesis, the appearance of the Schiff base, and metal structures are described as synthesized compounds. The IR results confirmed the bidentate nature of the Schiff's base ligand via hydroxy group oxygen and azomethane nitrogen. The presence of $-(\text{C}=\text{N}-)$ and $-\text{OH}$ bonds in the ligand are confirmed by IR spectra. Based on spectral studies. The Schiff's base ligand was coordinated to Co (II) and Cu (II) metal ions via O and N atoms to afford the corresponding complexes. The Schiff's base ligand its metal (II) complexes, $[\text{M}(\text{L})_2]$ (M=Co and Cu), were successfully synthesized and characterized. The

deprotonated bidentate Schiff base ligand coordinated to the metal (II) ion via -N=N- and -N-OH, resulting in a stable chelate ring. The metal (II) complexes show better antibacterial properties than the parent Schiff base ligand under similar experimental conditions. This study also concluded that the antibacterial growth inhibition ability of the synthesized compounds increased with increasing concentration.

Acknowledgment

We greatly appreciate the Delhi University, Jiwaji University, and Privi organics ltd, Mumbai for recording the spectral data.

References

1. M. Debdulal, IJRJAR, **6**, 471 (2019).
2. J. Sharma, P. Dogra1, N. Sharma, and Ajay - *AIP Conf. Proc.* (2019) pp. 2142.
3. C. Irawan, L. Nur, B. Mellisani, Arinzani, and Hanafi, *Rasayan J. Chem.* **12**, 951 (2019).
<https://doi.org/10.31788/RJC.2019.1225063>
4. S. A. Dalia, F. Afsan, M. S. Hossain, M. N. Khan, C. M Zakaria, M. Kudrat-E-Zahan, and M. M. Ali, *IJCS* **6**, 2859 (2018).
5. A. M. Whyte, R. Henderson, D. K. Henderson, P. A. Tasker, M. M. Matsushita, K. Awaga, F. J. White, P. Richardson, and N. Robertson, *Inorg. Chem.* **50**, 12867 (2011).
<https://doi.org/10.1021/ic2020644>
6. A. W. Ashbrook, *Coord. Chem. Rev.* **16**, 285 (1975).
[https://doi.org/10.1016/S0010-8545\(00\)80438-5](https://doi.org/10.1016/S0010-8545(00)80438-5)
7. N. Turan and K. Buldurun, *Eur. J. Chem.* **9**, 22 (2018).
<https://doi.org/10.5155/eurjchem.9.1.22-29.1671>
8. H. S. Çalik, E. Ispir, Ş. Karabuga, and M. Aslantas, *J. Organomet. Chem.* **801**, 122 (2016).
<https://doi.org/10.1016/j.jorganchem.2015.10.028>
9. H. Laila, A. Rahman, M. Ahmed, Abu-Dief, M. Rafat, El-Khatib, S. M. Abdel-Fatah, and A. A. Seleem, *Int. J. Nano. Chem.* **2**, 83 (2016). <https://doi.org/10.18576/ijnc/020303>
10. A. B. Thomas, R. K. Nanda, L. P. Kothapalli, and S. C. Hamane, *Arab. J. Chem.* **9**, S79 (2016).
<https://doi.org/10.1016/j.arabj.2011.02.015>
11. Y. -T. Liu, J. Sheng, D. -W. Yin, H. Xin, X. -M. Yang, Q. -Y. Qiao, and Z. -J. Yang, *J. Organomet. Chem.* **856**, 27 (2018). <https://doi.org/10.1016/j.jorganchem.2017.12.022>
12. M. Lashanzadegan, S. Shayegan, and M. Sarkheil, *J. Serbian Chem. Soc.* **81**, 153 (2016).
<https://doi.org/10.2298/JSC150708085L>
13. H. Yu, W. Zhang, Q. Yu, F.-P. Huang, H.-D. Bian, and H. Liang, *Molecules* **22**, ID 1772 (2017). <https://doi.org/10.3390/molecules22101772>
14. K. Lekaa and A. K. Areal, *J. Pharm. Sci. Res.* **10**, 1912 (2018).
15. G. Valarmarhy, R. Subbalakshmi, R. Renganathan, and R. Kokila, *AJOC* **30**, 645 (2018).
16. Z. -J. Yao, K. Li, J. -Y. Zhang, Y. Wang, and W. Deng, *Inorg. Chim. Acta* **450**, 118 (2016).
<https://doi.org/10.1016/j.ica.2016.05.032>
17. A. S. Shekhawat, N. S. Chundawat, N. P. Singh, and G. P. Singh, *Sci. Technol. Development* **10**, 572 (2021).
18. M. Y. Wani, S. Kumar, C. T. Arranja, Dias, C. M. F. Dias, and A. J. F. N. Sobral, *New J. Chem.* **40**, 4974 (2016). <https://doi.org/10.1039/C5NJ03198B>
19. P. Rathii and D. P. Singh, *Acta Mol. Biomol. Spectros.* **128**, 243 (2015).
20. M. Shebl, *Spectrochimica Acta* **117**, 127 (2014). <https://doi.org/10.1016/j.saa.2013.07.107>
21. L. H. Abdel-Rahman, A. M. Abu-Dief, R. M. El-Khatib, and S. M. Abdel-Fatah, *J. Photochem. Photobiol. B* **162**, 298 (2016). <https://doi.org/10.1016/j.jphotobiol.2016.06.052>